

### Smooth Fourier interpolation of periodic functions

Warren E. Pickett

*Condensed Matter Physics Branch, Naval Research Laboratory, Washington, D.C. 20375-5000*

Henry Krakauer

*Department of Physics, College of William and Mary, Williamsburg, Virginia 23185*

Philip B. Allen

*Department of Physics, State University of New York, Stony Brook, New York 11794-3800*

(Received 22 February 1988)

The Shankland-Koelling-Wood Fourier interpolation scheme is altered by a more physical choice of roughness function. Examples are presented demonstrating the improvement in the resulting band-structure plots; a more critical application is to the computation of the transport properties of crystalline solids which require second derivatives of the electronic energy bands.

Shankland<sup>1</sup> introduced a method by which a periodic function known at discrete set of points can be represented by a Fourier series which passes *exactly* through the given points and yet *remains smooth*. Koelling and Wood<sup>2</sup> verified that the method was viable and illustrated several characteristics of the procedure. In this paper we point out a refinement of their implementation which can be important, especially if accurate first and second derivatives of the interpolation function are desired.

We consider the interpolation of  $N$  one-electron eigenvalues  $\epsilon(\mathbf{k}_i)$  in a three-dimensional periodic solid. A Fourier-series interpolation is employed, and the space-group symmetry is incorporated by using "star functions"  $S_m(\mathbf{k})$ .<sup>2</sup> The interpolation function is written

$$\tilde{\epsilon}(\mathbf{k}) = \sum_{m=1}^M \epsilon_m S_m(\mathbf{k}), \tag{1}$$

and the idea is to use *more expansion coefficients*  $\epsilon_m$  *than data points* ( $M > N$ ). The interpolation function is required to pass precisely through all data points, with the remaining freedom in the coefficients optimized to minimize the roughness according to some given definition.

The mathematical problem is to minimize the roughness  $\mathcal{R}$  subject to the  $N$  constraints

$$\tilde{\epsilon}(\mathbf{k}_i) = \epsilon(\mathbf{k}_i). \tag{2}$$

The sole difference in our implementation of this interpretation procedure is in the choice of roughness function. Koelling and Wood<sup>2</sup> considered the form

$$\begin{aligned} \mathcal{R} &= \frac{1}{N_k} \sum_{\mathbf{k}} \{ C_0 \tilde{\epsilon}(\mathbf{k}) + C_1 |\nabla \tilde{\epsilon}(\mathbf{k})|^2 + C_2 |\nabla^2 \tilde{\epsilon}(\mathbf{k})|^2 + \dots \} \\ &= \sum_{m=1}^M |\epsilon_m|^2 \rho(R_m), \end{aligned} \tag{3}$$

where  $N_k$  is the number of  $\mathbf{k}$  points in the Brillouin zone,  $R_m = |\mathbf{R}_m|$  is the length of the lattice vectors in the  $m$ th star, and

$$\rho(R_m) = C_0 + C_1 R_m^2 + C_2 R_m^4 + \dots \tag{4}$$

This expression for  $\rho$  follows from the definition of the star function

$$S_m(\mathbf{k}) = \frac{1}{n} \sum_{\Lambda} e^{i\mathbf{k} \cdot \Lambda \mathbf{R}_m}, \tag{5}$$

where  $\{\Lambda\}$  are the  $n$  point-group rotations in the space group, and from orthogonality relations involving Brillouin zone (BZ) summations. The form (3) has the undesired effect of minimizing (with relative weight  $C_0$ ) excursions of the function  $\tilde{\epsilon}(\mathbf{k})$  from zero, whereas the more physical restriction is to minimize the excursions of  $\tilde{\epsilon}(\mathbf{k})$  from its mean value  $\epsilon_1$ . (Stars are ordered such that  $R_m$  is nondecreasing as  $m$  increases;  $R_1 = 0$ .) This is readily taken into account by omitting the  $m = 1$  term from the sum in Eq. (3)

$$\mathcal{R} = \sum_{m=2}^M |\epsilon_m|^2 \rho(R_m), \tag{6}$$

since the  $m = 1$  contributions proportional to  $C_1$  and  $C_2$  [derivatives of  $\tilde{\epsilon}(\mathbf{k})$ ] vanish because  $R_1 = 0$ .

Minimizing  $\mathcal{R}$  in Eq. (6) subject to the constraints (2) similar to the procedure of Koelling and Wood leads to the set of linear equations

$$\epsilon_m^* \rho_m = \sum_{i=1}^N \lambda_i S_m(\mathbf{k}_i), \quad m > 1, \tag{7}$$

$$0 = \sum_{i=1}^N \lambda_i, \tag{8}$$

together with the constraints of Eq. (2). Here  $\rho_m$  is defined as  $\rho(R_m)$ . Since the formalism becomes different from that of Koelling and Wood, we give a brief description. Choosing a particular data point, say  $i = N$ , Eq. (8) can be solved for  $\lambda_N$  and incorporated into (7) to give

$$\epsilon_m^* \rho_m = \sum_{i=1}^{N-1} \lambda_i [S_m(\mathbf{k}_i) - S_m(\mathbf{k}_N)]. \tag{9}$$

Multiplying the complex conjugate of (9) by  $[S_m(\mathbf{k}_j) - S_m(\mathbf{k}_N)]/\rho_m$  and summing  $m$  from 2 to  $M$  gives

$$\Delta\epsilon_j \equiv \epsilon(\mathbf{k}_j) - \epsilon(\mathbf{k}_N) = \sum_{i=1}^{N-1} H_{ji} \lambda_i^*, \quad (10)$$

where

$$H_{ji} = \sum_{m=2}^M \frac{[S_m(\mathbf{k}_j) - S_m(\mathbf{k}_N)][S_m^*(\mathbf{k}_i) - S_m^*(\mathbf{k}_N)]}{\rho_m}. \quad (11)$$

Solving (10) for  $\lambda_i$ , the expansion coefficients are given by

$$\epsilon_m = \rho_m^{-1} \sum_{i=1}^{N-1} \lambda_i^* [S_m^*(\mathbf{k}_i) - S_m^*(\mathbf{k}_N)], \quad m < 1, \quad (12a)$$

$$\epsilon_1 = \epsilon(\mathbf{k}_N) - \sum_{m=2}^M \epsilon_m S_m(\mathbf{k}_N). \quad (12b)$$

The improvement resulting from the omission of the  $m=1$  star from the roughness function was discovered while calculating transport coefficients<sup>3</sup> for the  $\text{La}_{2-x}\text{M}_x\text{CuO}_4$  ( $M=\text{Sr}, \text{Ba}$ ) superconducting oxide system. To define an appropriate roughness function, we noted that at the top of the band where  $\epsilon(\mathbf{k}) - \epsilon_1 > 0$ , the second derivative  $\nabla^2\epsilon(\mathbf{k})$  should be predominantly negative, and the roughness is reduced most effectively by minimizing some combination of  $\epsilon(\mathbf{k}) - \epsilon_1$  and  $\nabla^2\epsilon(\mathbf{k})$ . At the bottom of the band where  $\epsilon(\mathbf{k}) - \epsilon_1 < 0$ ,  $\nabla^2\epsilon(\mathbf{k})$  should be encouraged to be positive. These considerations are symmetric around the band center and can be accomplished by minimizing  $[\epsilon(\mathbf{k}) - \epsilon_1 + C_1 \nabla^2\epsilon(\mathbf{k})]^2$ , with  $C_1$  positive. The roughness function which results, whose overall scale is irrelevant,<sup>2</sup> is given by Eq. (6) with  $\rho$  given by

$$\rho_m = (1 - C_1 X_m^2)^2 + C_2 X_m^6, \quad (13)$$

where  $X_m = R_m/R_{\min}$  and  $R_{\min}$  is the smallest nonzero lattice vector. The  $X_m^6$  term will help to suppress small-amplitude, short-wavelength wiggles.

The relevant band in  $\text{La}_2\text{CuO}_4$  (band 17, which crosses the Fermi level) is shown in Fig. 1. Since the conducti-

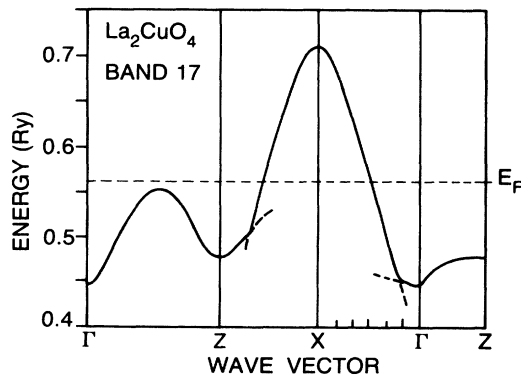


FIG. 1. Band 17 in  $\text{La}_2\text{CuO}_4$  along symmetry directions. Kinks occur in the bands at band crossings, which are indicated by dashed lines.

ty involves band velocity  $\nabla\epsilon(\mathbf{k})$  and the Hall coefficient requires the inverse band mass tensor  $\nabla\nabla\epsilon(\mathbf{k})$  as well, it was necessary to establish that the first and second derivatives of the interpolation function (1) give reasonable results. Using 135 equally spaced first-principles eigenvalues, the Koelling-Wood scheme using 679 stars leads to the curvatures (second derivatives) plotted in Fig. 2(a). Evidently there are oscillations, such as near the X point, which are unphysical and would lead to uncertainties in the zone sum, although the general behavior is correct. Upon increasing the number of stars to 970, the only noticeable change occurs near the  $\Gamma$  point along  $X-\Gamma$ , and this change is small.

The effect of omitting the  $R=0$  ( $m=1$ ) term in the roughness function results in the curvatures plotted in

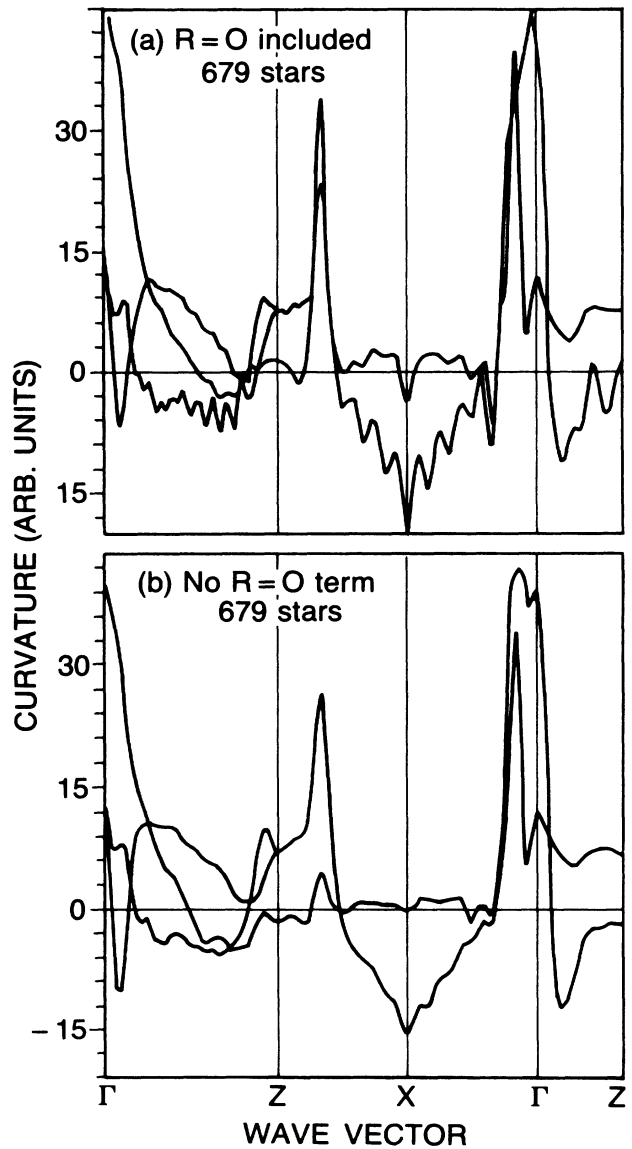


FIG. 2. Various curvatures of the band shown in Fig. 1. (a) Results obtained using the Koelling-Wood roughness function including the  $R=0$  term. (b) Results obtained by omitting the  $R=0$  term from the roughness functions.

Fig. 2(b). Not only is the unphysical oscillation greatly reduced (as occurs over most of the lowest curve) but other behavior becomes more regular. This is evident particularly for the upper curve near  $X$ , as well as for the lower band near  $Z$  which changes sign when the  $m = 1$  term is omitted. Again, increasing the number of stars (fitting parameters) to 970 produces no significant change. Figure 2(b) resulted from values  $C_1 = C_2 = 0.25$  in Eq. (13). Tests with  $C_1 = C_2 = 0.05$  and  $C_1 = C_2 = 0.75$  also produced no noticeable change, consistent with the finding of Koelling and Wood that the fit is very insensitive to the magnitudes of the constants in the roughness function.

We note one other feature (which may not be related to the specifics of the roughness function) which reflects favorably on the Shankland-Koelling-Wood (SKW) scheme. It is known that band crossings in multiband systems, which induce nonanalytic kinks in a given band, can lead to "ringing," i.e., oscillations which extend well away from the kink. In Fig. 1 two kinks can be seen, with small sections of the next lower band shown by dashed lines. Complete band plots (given in Ref. 4) demonstrate that the Fourier series does a good job of approximating these kinks. To investigate the importance of possible "ringing" effects, the first-principles  $k$  points

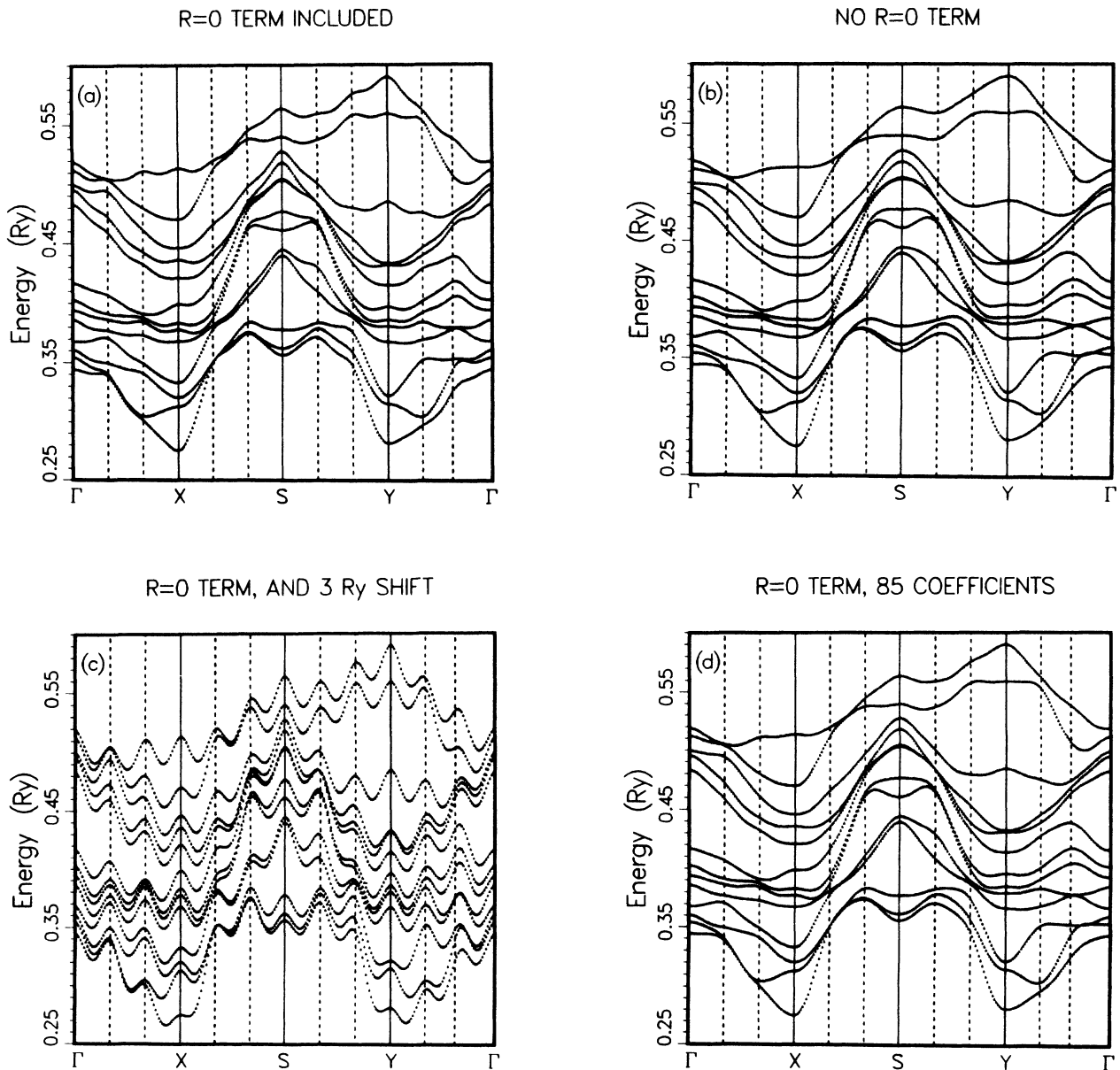


FIG. 3. Band structure plots along high symmetry directions in the basal plane ( $k_z = 0$ ) for a model  $\text{YBa}_2\text{Cu}_3\text{O}_7$  compound (non-self-consistent). Curves are constrained to pass exactly through the calculated eigenvalues at the high symmetry points  $\Gamma$ ,  $Y$ ,  $S$ , and  $X$  and at the intermediate points denoted by vertical dashed lines. (a) Shankland-Koelling-Wood method. (b) Modification with  $R = 0$  term excluded from the roughness function. (c) Results from rigid shifting of bands as described in the text. (d) Shankland-Koelling-Wood method, but using only 85 Fourier coefficients, similar to conventional practice.

nearest the two kinks were omitted from the data and the Fourier coefficients were redetermined. Although the curvature near the kinks was drastically reduced (as expected), well away from the kinks the change in curva-

ture was negligible. This indicates the curvature resulting from interpolation is determined locally, as desired. As a result, velocities and curvatures on the Fermi surface are not influenced inordinately by band crossings as

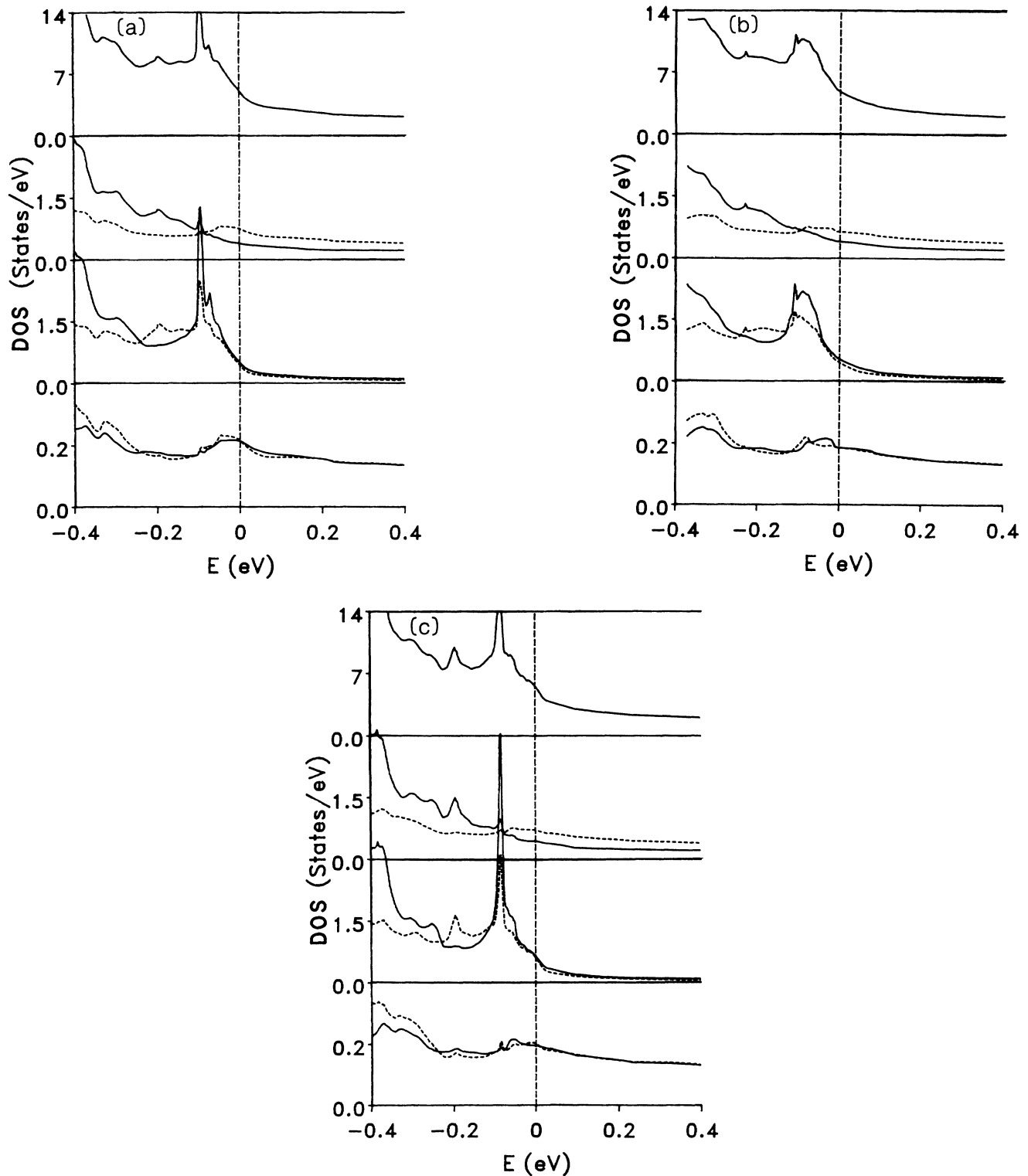


FIG. 4. Density of states (DOS) near the Fermi level (taken as the zero of energy) for  $\text{YBa}_2\text{Cu}_3\text{O}_7$ : top panel, total DOS; second panel, the two distinct copper sites; third panel, the chain-related oxygen sites; bottom panel, layer-related oxygen sites. (a) Straight tetrahedron method based on 147 *ab initio* points. (b) SKW method. (c) Modified SKW method.

long as they do not occur very near the Fermi level.

As another example of the difference resulting from our modifications, we provide a case in which the difference in the expansion procedure can be seen in the bands themselves. The system we choose is a model<sup>5</sup> of  $\text{YBa}_2\text{Cu}_3\text{O}_7$ , a complicated crystal which has orthorhombic  $Pmnm$  space-group symmetry. Each interpolation of the bands is based on the same 32 first-principles  $\mathbf{k}$  points and 416 expansion coefficients. The bands in Fig. 3(a) were calculated using the SKW procedure, while those in Fig. 3(b) resulted from the present modification. To illustrate more graphically the undesirable results which can occur from including the  $R=0$  term, we shifted the first-principles eigenvalues upward rigidly by 3 Ry, carried out the SKW procedure, and then shifted the resulting bands downward rigidly by 3 Ry, obtaining the bands shown in Fig. 3(c). In each of Figs. 3(a)–3(c) the vertical dashed lines indicate the positions of the calculated input eigenvalues (identical for each case).

From Fig. 3(b) it is clear that eliminating the  $R=0$  term results in smooth bands, in spite of using over an order of magnitude more Fourier coefficients than calculated points. The SKW procedure results in bands which display additional wiggles [Fig. 3(a)], typically near the input points, which are reproduced exactly in each case. Figure 3(c) illustrates in an exaggerated way what is occurring: Between each of the input points the freedom afforded by the large number of Fourier coefficients is being used to *minimize the band energy*  $\epsilon(\mathbf{k})$ , rather than the magnitude of its curvature or its distance from the average band position. This “drooping” of the bands from the input (constrained) points is exaggerated by shifting the input eigenvalues upward before determining the Fourier coefficients. This last feature also graphically illustrates the undesirable dependence of the results of the SKW procedure on the energy scale itself (that is, an additive constant), a dependence which is eliminated by omitting the  $R=0$  term in Eq. (3).

The unacceptable results of Fig. 3(c) would not occur in most applications of the SKW scheme as applied in the past, since it is not the practice to use more than 2–3 times more expansion coefficients than input eigenvalues. This is illustrated in Fig. 3(d), where the SKW scheme is applied with only 85 coefficients rather than 416 as in Figs. 3(a)–(c). The resulting bands are fairly smooth, although not quite as smooth as obtained using our modified scheme with equal variational freedom. In trying to get smooth velocities and curvatures, however, it is natural to increase the variational freedom of the Fourier representation, and Fig. 3(c) illustrates a pitfall. In recent work we have found it useful to generate realistic densities of states (DOS) for several model (i.e., non-self-consistent) systems<sup>5</sup> with large unit cells, and this is much

more efficient if only a relatively small number of  $\mathbf{k}$  points need to be calculated. Cases have been encountered in which the SKW scheme gives unacceptably poor DOS curves, whereas the present modification has been reliable.

As an illustration of how our modification can affect critical point structure in density of states calculations, we present in Fig. 4 results near the Fermi level from our self-consistent linearized augmented plane-wave (LAPW) studies<sup>6</sup> of the high-temperature superconductor  $\text{YBa}_2\text{Cu}_3\text{O}_7$ . These results are all based on 147 input  $\mathbf{k}$  points in the irreducible Brillouin zone, which represents a rather fine mesh for such a large unit cell (small Brillouin zone). In Fig. 4(a) these 147 points are used directly in the linear tetrahedron scheme<sup>7</sup> without the use of any Fourier interpolation whatever. Figures 4(b) and 4(c) show the results of the SKW method and our modification, respectively, with 2123 expansion coefficients used in each case. The tetrahedron method is used with 400 extrapolated  $\mathbf{k}$  points (which corresponds to 2527  $\mathbf{k}$  points and 11 664 tetrahedrons in the full Brillouin zone). The structure of the oxygen-related peak at approximately  $-0.1$  eV is smeared by the SKW procedure, indicating that superfluous wiggles have been introduced into a band which is very flat when our method is applied. Direct tetrahedral integration [Fig. 4(a)] of the original 147 points reproduces this critical structure better than the SKW scheme.

In summary, we have presented a variation of the Shankland<sup>1</sup>-Koelling-Wood<sup>2</sup> interpolation scheme which incorporates a more physical definition of roughness. Numerical tests indicate curvatures are greatly improved. Even the appearance of plotted bands can be changed appreciably, and certain sensitive properties such as the density of states near critical points should also be improved.

#### ACKNOWLEDGMENTS

We are grateful to D. D. Koelling for comments on the manuscript. The work of W. E. Pickett was supported by the Office of Naval Research; H. Krakauer was supported by the National Science Foundation under Grant No. DMR-84-16046; and P. B. Allen acknowledges a sabbatical stay at the Naval Research Laboratory funded by an Intergovernmental Personnel Act Grant, and partial support by the National Science Foundation under Grant No. DMR-84-20708. Computations were carried out under the auspices of the National Science Foundation at the Cornell National Superconductor Facility and at the Pittsburgh Supercomputer Center, as well as on the Naval Research Laboratory CRAY X/MP.

<sup>1</sup>D. G. Shankland, in *Computational Methods in Band Theory*, edited by P. Marcus, J. Janak, and A. Williams (Plenum, New York, 1971), p. 362.

<sup>2</sup>D. D. Koelling and J. H. Wood, *J. Comput. Phys.* **67**, 253 (1986).

<sup>3</sup>P. B. Allen, W. E. Pickett, and H. Krakauer, *Phys. Rev. B* **36**, 3926 (1987).

<sup>4</sup>H. Krakauer, W. E. Pickett, D. A. Papaconstantopoulos, and L. L. Boyer, *Jpn. J. Appl. Phys.* **26**, 991 (1987).

<sup>5</sup>The first-principles eigenvalues used in preparing Fig. 3 were

taken from a linearized augmented plane-wave calculation in which the one-electron potential for  $\text{YBa}_2\text{Cu}_3\text{O}_7$  was calculated from overlapping spherical ionic charge densities. This is not a self-consistent result, so the bands of Fig. 3 should not be expected to correspond to any other published band struc-

ture of  $\text{YBa}_2\text{Cu}_3\text{O}_7$ .

<sup>6</sup>H. Krakauer, W. E. Pickett, and R. E. Cohen, *J. Supercon.* **1**, 111 (1988).

<sup>7</sup>G. Lehmann and M. Taut, *Phys. Status Solidi B* **54**, 469 (1972).